01 Nov 2022

# Conservative Unconditionally Stable Decoupled Numerical Schemes for the Cahn–Hilliard–Navier–Stokes–Darcy–Boussinesq System

Wenbin Chen

Daozhi Han
*Missouri University of Science and Technology*, handaoz@mst.edu

Xiaoming Wang

Yichao Zhang



## Recommended Citation

W. Chen et al., "Conservative Unconditionally Stable Decoupled Numerical Schemes for the Cahn–Hilliard–Navier–Stokes–Darcy–Boussinesq System," *Numerical Methods for Partial Differential Equations*, vol. 38, no. 6, pp. 1823 - 1842, Wiley, Nov 2022.
The definitive version is available at https://doi.org/10.1002/num.22841

Received: 4 January 2021 | Revised: 17 June 2021 | Accepted: 30 June 2021 | Published on: 10 September 2021

DOI: 10.1002/num.22841



RESEARCH ARTICLE

WILEY

# Conservative unconditionally stable decoupled numerical schemes for the Cahn–Hilliard–Navier–Stokes–Darcy–Boussinesq system

**Wenbin Chen**[1] | **Daozhi Han**[2] | **Xiaoming Wang**[3] | **Yichao Zhang**[4]

[1]School of Mathematical Sciences, Shanghai Key Laboratory of Mathematics for Nonlinear Sciences, Fudan University, Shanghai, China
[2]Department of Mathematics and Statistics, Missouri University of Science and Technology, Rolla, Missouri, USA
[3]Department of Mathematics, SUSTech International Center for Mathematics, National Center for Applied Mathematics Shenzhen, Guangdong Provincial Key Laboratory of Computational Science and Material Design, Southern University of Science and Technology, Shenzhen, China
[4]School of Mathematical Sciences, Fudan University, Shanghai, China

**Correspondence**
Xiaoming Wang, Department of Mathematics, and National Center for Applied Mathematics Shenzhen (NaCAMS), Southern University of Science and Technology, Shenzhen, China.
Email: wxm.math@outlook.com

**Funding information**
Wenbin Chen is supported by the National Key R&D Program of China (2019YFA0709502) and NSFC (12071090). Daozhi Han acknowledges support from NSF-DMS-1912715. Xiaoming Wang thanks support from NSFC (11871159) and Guangdong Provincial Key Laboratory of Computational Science and Material Design (2019B030301001). Dedicated to Max Gunzburger on the occasion of his 75th birthday.

## Abstract

We propose two mass and heat energy conservative, unconditionally stable, decoupled numerical algorithms for solving the Cahn–Hilliard–Navier–Stokes–Darcy–Boussinesq system that models thermal convection of two-phase flows in superposed free flow and porous media. The schemes totally decouple the computation of the Cahn–Hilliard equation, the Darcy equations, the heat equation, the Navier–Stokes equations at each time step, and thus significantly reducing the computational cost. We rigorously show that the schemes are conservative and energy-law preserving. Numerical results are presented to demonstrate the accuracy and stability of the algorithms.

**KEYWORDS**

convection, phase field model, two-phase flow, unconditional stability

# 1 | INTRODUCTION

## 1.1 | The mathematical model

We investigate efficient schemes for the Cahn–Hilliard–Navier–Stokes–Darcy–Boussinesq system (CHNSDB) for thermal convection of two-phase flows in a fluid layer overlying a porous media as formulated in Chen et al. [1]. Since the problem involves two different fluid regions, we first fix some notation. Assume that $\Omega \in \mathbb{R}^d$ $(d = 2, 3)$ is a bounded connected domain of smooth boundary. The domain $\Omega$ is split into two non-overlapping regions $\Omega_c, \Omega_m$ such that $\overline{\Omega} = \overline{\Omega}_c \cup \overline{\Omega}_m$ and $\Omega_c \cap \Omega_m = \emptyset$. $\Omega_c$ represents the fluid layer where the fluids are subject to the Navier–Stokes equation, and $\Omega_m$ represents the porous media where Darcy flow dominates the region. We denote $\partial\Omega_c$ and $\partial\Omega_m$ the boundaries of $\Omega_c$ and $\Omega_m$ respectively. The domain interface between the two regions is denoted by $\Gamma_{cm}$, on which $\mathbf{n}_{cm}$ denotes the unit normal to $\Gamma_{cm}$ pointing from $\Omega_c$ to $\Omega_m$. We also denote $\Gamma_c = \partial\Omega_c \backslash \Gamma_{cm}$ and $\Gamma_m = \partial\Omega_m \backslash \Gamma_{cm}$ with $\mathbf{n}_c, \mathbf{n}_m$ being the unit outer normals to $\Gamma_c$ and $\Gamma_m$. On the interface $\Gamma_{cm}$, we denote by $\{\boldsymbol{\tau}_i\}$ $(i = 1, \ldots, d-1)$ a local orthonormal basis for the tangent plane to $\Gamma_{cm}$. A two dimensional geometry is shown in Figure 1 for illustration.

We denote by $\mathbf{u}$ the fluid velocity, $\varphi$ the phase field function and $T$ the overall temperature. Furthermore, variables are distinguished by their subscripts ($m$ or $c$) indicating where the variables operate, that is, for $j \in \{c, m\}$

$$\mathbf{u}|_{\Omega_j} = \mathbf{u}_j, \quad \varphi|_{\Omega_j} = \varphi_j, \quad T|_{\Omega_j} = T_j.$$

The CHNSDB system reads as follows:

$$\rho_0(\partial_t \mathbf{u}_c + (\mathbf{u}_c \cdot \nabla)\mathbf{u}_c) - \nabla \cdot (2\nu(\varphi_c, T_c)\mathbb{D}(\mathbf{u}_c)) + \nabla P_c + \varphi_c \nabla \mu_c = \alpha\rho_0 g(T_c - \overline{T})\vec{z}, \quad \text{in } \Omega_c, \tag{1}$$

$$\frac{\rho_0}{\chi}\partial_t \mathbf{u}_m + \nu(\varphi_m, T_m)\Pi^{-1}\mathbf{u}_m + \nabla P_m + \varphi_m \nabla \mu_m = \alpha\rho_0 g(T_m - \overline{T})\vec{z}, \quad \text{in } \Omega_m, \tag{2}$$

$$\nabla \cdot \mathbf{u}_j = 0, \quad \text{in } \Omega_j, \tag{3}$$

$$\partial_t T_j + \mathbf{u}_j \cdot \nabla T_j = \nabla \cdot (\kappa_j(T_j)\nabla T_j), \quad \text{in } \Omega_j, \tag{4}$$

$$\partial_t \varphi_j + \nabla \cdot (\mathbf{u}_j \varphi_j) = \operatorname{div}(M(\varphi_j)\nabla \mu_j), \quad \text{in } \Omega_j, \tag{5}$$

$$\mu_j = \gamma\left[\frac{1}{\varepsilon}(\varphi_j^3 - \varphi_j) - \varepsilon\Delta\varphi_j\right], \quad \text{in } \Omega_j. \tag{6}$$

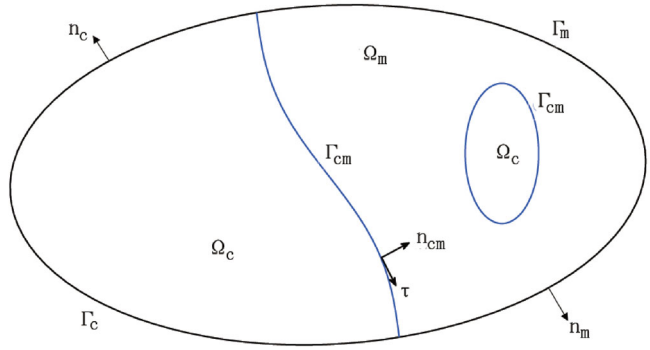


FIGURE 1 A 2D illustration of the domain

where $j \in \{c, m\}$, $\mathbb{D}(\mathbf{u}_c)$ is the rate of strain tensor $\mathbb{D}(\mathbf{u}_c) = \frac{1}{2}(\nabla \mathbf{u}_c + \nabla^T \mathbf{u}_c)$. Here $\rho_0$ is the fluid density, $\alpha$ is the thermal expansion coefficient and $\overline{T}$ is the average temperature, $g$ is the gravitational acceleration, $\vec{z}$ is the unit vector pointing in the inverse direction of gravity, M denotes the mobility, $\chi$ is the porosity and $\Pi$ is the permeability matrix of size $d \times d$, $\nu$ is the dynamic viscosity depending on phase field function $\varphi$ and temperature $T$, $\kappa$ is the thermal diffusivity of the fluid mixture dependent on temperature $T$, $\mu$ is the chemical potential and $\gamma$ is a positive parameter related to the surface tension. We assume that the viscosity $\nu$, thermal diffusivity $\kappa$ and mobility $M$ are suitable functions such that $0 < \overline{c} \le \nu, \kappa, \mathrm{M} \le \overline{C}$ for positive constants $\overline{c}$ and $\overline{C}$.

The CHNSDB system is subject to the following boundary and interface conditions.

Boundary conditions on $\Gamma_c$ and $\Gamma_m$:

$$\mathbf{u}_c = \mathbf{0}, \quad \frac{\partial \mathrm{T}_c}{\partial \mathbf{n}_c} = \frac{\partial \varphi_c}{\partial \mathbf{n}_c} = \frac{\partial \mu_c}{\partial \mathbf{n}_c} = 0, \quad \text{on } \Gamma_c, \tag{7}$$

$$\mathbf{u}_m \cdot \mathbf{n}_m = 0, \quad \frac{\partial \mathrm{T}_m}{\partial \mathbf{n}_m} = \frac{\partial \varphi_m}{\partial \mathbf{n}_m} = \frac{\partial \mu_m}{\partial \mathbf{n}_m} = 0, \quad \text{on } \Gamma_m. \tag{8}$$

Interface conditions on $\Gamma_{cm}$:

$$\varphi_m = \varphi_c, \quad \frac{\partial \varphi_m}{\partial \mathbf{n}_{cm}} = \frac{\partial \varphi_c}{\partial \mathbf{n}_{cm}}, \quad \text{on } \Gamma_{cm}, \tag{9}$$

$$\mu_m = \mu_c, \quad M(\varphi_m)\frac{\partial \mu_m}{\partial \mathbf{n}_{cm}} = M(\varphi_c)\frac{\partial \mu_c}{\partial \mathbf{n}_{cm}}, \quad \text{on } \Gamma_{cm}, \tag{10}$$

$$T_m = T_c, \quad \kappa_m \frac{\partial T_m}{\partial \mathbf{n}_{cm}} = \kappa_c \frac{\partial T_c}{\partial \mathbf{n}_{cm}}, \quad \text{on } \Gamma_{cm}, \tag{11}$$

$$\mathbf{u}_m \cdot \mathbf{n}_{cm} = \mathbf{u}_c \cdot \mathbf{n}_{cm}, \quad \text{on } \Gamma_{cm}, \tag{12}$$

$$-2\nu(\varphi_c)\mathbf{n}_{cm} \cdot (\mathbb{D}(\mathbf{u}_c)\mathbf{n}_{cm}) + P_c + \frac{1}{2}\rho_0 |\mathbf{u}_c|^2 = P_m, \quad \text{on } \Gamma_{cm}, \tag{13}$$

$$-\tau_i \cdot (\mathbb{D}(\mathbf{u}_c)\mathbf{n}_{cm}) = \frac{\alpha_{\mathrm{BJSJ}}}{2\sqrt{\mathrm{trace}(\Pi)}}\tau_i \cdot \mathbf{u}_c, \quad i = 1, \ldots, d-1, \text{on } \Gamma_{cm}, \tag{14}$$

where $\alpha_{\mathrm{BJSJ}}$ is a parameter in the Beavers–Joseph–Saffman–Jones (BJSJ) condition. Here $\alpha_{\mathrm{BJSJ}}$ is assumed to be a non-negative constant for simplicity.

There are two important identities associated with the CHNSDB system (1)–(6) under the boundary and interface boundary conditions (7)–(14): an energy law and heat conservation-both established in Chen et al. [1]. To introduce the energy law, we let $\lambda$ be an upper bound of the largest eigenvalue of $\Pi$, and $C_p, C_k > 0$ be the coefficients such that

$$\|T - \overline{T}\|^2_{L^2(\Omega)} \le C_p \|\nabla T\|^2_{L^2(\Omega)}, \qquad \|\mathbf{u}_c\|^2_{L^2(\Omega_c)} \le C_k \|\mathbb{D}(\mathbf{u}_c)\|^2_{L^2(\Omega_c)}. \tag{15}$$

For any constant A such that

$$A \ge \max\left\{ \frac{C_p C_k (\alpha \rho_0 g)^2}{8\overline{c}^2}, \frac{C_p \lambda (\alpha \rho_0 g)^2}{4\overline{c}^2} \right\}, \tag{16}$$

we define the total energy of the system as

$$\mathcal{E}_A(t) := \int_{\Omega_c} \frac{\rho_0}{2}|\mathbf{u}_c|^2 dx + \int_{\Omega_m} \frac{\rho_0}{2\chi}|\mathbf{u}_m|^2 dx + A\int_{\Omega} \frac{1}{2}T^2 dx + E(\varphi), \tag{17}$$

where $E(\varphi) := \gamma \int_\Omega \left[\frac{\varepsilon}{2}|\nabla\varphi|^2 + \frac{1}{\varepsilon}F(\varphi)\right] dx$ is the total free energy, and $F(\varphi) = \frac{1}{4}(\varphi^2-1)^2$ is a double-well potential. Then the following identities hold

$$\frac{d}{dt}\mathcal{E}_A(t) \le 0, \quad \frac{d}{dt}\int_\Omega T dx = 0, \quad \forall t \ge 0. \tag{18}$$

Due to the conservation of the total heat energy, one can shift the temperature $T$ by its average value $\overline{T}$

$$T^* = T - \overline{T}, \quad T_c^* = T_c - \overline{T}, \quad T_m^* = T_m - \overline{T}.$$

so that $T^*$ is of zero mean. The CHNSDB system (1)–(6) can then be equivalently expressed in terms of $T^*$. From now on, we shall assume that the temperature has zero mean and retain the notation $T$ in place of $T^*$.

### 1.2 | Previous works

Flows in a fluid layer overlying a porous media see important applications in contaminant transport in karst aquifers, cardiovascular modeling and simulation, oil recovery, and in understanding the hydrodynamic and biochemical processes in hyporheic zone under a river bed [2], to name a few. In the past decade intense research has been directed at the study of single phase flow in the coupled free flow and porous media, compare References [3–9] among many others. Of particular interest in this context are the phenomena of thermal convection in a fluid layer overlying a porous medium that has been intensively studied by a number of authors in recent years [10–22]. The modeling of two-phase flows in this setting is relatively new. A hybrid of a sharp interface model in porous media and a diffuse interface model in the free flow is proposed in Chen et al. [23]. In Han et al. [24] we systematically derived the Cahn–Hilliard–Stokes–Darcy model (CHSD) for two-phase flows in coupled conduit and porous media based on Onsager's extremum principle and the diffuse interface formalism. Well-posedness of the CHSD system is considered in Han et al. [25]. The CHNSDB model (1)–(14) is recently introduced in Chen et al. [1] for two-phase flows in superposed free flow and porous media taking into account of thermal convection and inertia effect of free flow.

There are two major challenges in solving the CHNSDB system. The first one is the stiffness associated with the diffusive interface between the two fluid components (sharp transition over a small layer)—an issue intrinsic to diffuse interface fluid models. This issue is usually handled by the design of energy-law preserving (hence unconditionally stable) numerical methods. Popular approaches include the convex-concave splitting [26–29], the invariant energy quadratization (Lagrange multiplier) method [30–33], and the scalar auxiliary variable (SAV) approach [34, 35]. We refer to References [36–45] for applications of these methods to diffuse interface fluid models. The second challenge is the multi-physics coupling governed by the Cahn–Hilliard equation, the Navier–Stokes equations, the Darcy equations, and the heat equation. Based on the ideas of operator splitting and pressure stabilization we designed a totally decoupled unconditionally stable numerical scheme in Chen et al. [46] for solving the CHSD system. The ideas are in turn inspired by those in References [46–49]. Extension of these ideas to the CHNSDB model leads to two uncoupled algorithms in a recent work [1].

It is important to note that the algorithms proposed in our earlier work [1] do not conserve the total heat energy. In addition, the fluid velocity and pressure are still coupled in the computation of the Navier–Stokes equations, resulting in a large linear system-especially in three dimension-to be solved. The main contribution of this article is the design of two conservative, unconditionally stable, decoupled numerical algorithms that allow for sequential uncoupling of the computation of the Cahn–Hilliard equation, the Darcy equations, the heat equation, and the Navier–Stokes

equations. To realize conservation of heat energy the first scheme employs a modified velocity in the convection-diffusion equation, while the second scheme undergoes a post-processing procedure for the temperature field. In addition, the computation of velocity and the update of pressure are also decoupled in the second scheme. We rigorously show that the schemes are mass and heat-energy conservative. We establish that the numerical methods satisfy modified discrete energy laws and are therefore unconditionally energy-stable. Properties of the schemes, including conservation, temporal accuracy, and stability are further validated through numerical experiments.

We point out that the idea for decoupling Cahn–Hilliard equation from fluid equation in this article does not seem to have a direct extension to second order scheme. Second order operator splitting method such as Strang splitting (cf. Zhao [50]) can be applied, though the splitting scheme may not satisfy an energy law. Recently developed SAV approach [51–54] is promising in the design of second order unconditionally stable decoupled time-marching scheme. Application of the SAV approach to our model with additional coupling via domain interface boundary conditions will be pursued in a future work. We note also that error analysis of our methods, though not carried out in this work, is possible, compare References [42, 55, 56] for the corresponding analysis in the case of single domains, and Chen et al. [57] for error analysis of a similar scheme in the setting of coupled domains.

The rest of the article is organized as follows. In Section 2 we present the schemes and prove that they are conservative and energy-law preserving. Numerical results are reported in Section 3. We conclude the article with a few remarks in Section 4.

## 2 | THE NUMERICAL SCHEME

### 2.1 | Preliminaries

We introduce the following function spaces

$$
\begin{aligned}
&\mathbf{H}(\mathrm{div};\Omega_j) \coloneqq \{\mathbf{w}\in\mathbf{L}^2(\Omega_j)\,|\nabla\cdot\mathbf{w}\in\mathbf{L}^2(\Omega_j)\}, \qquad j\in\{c,m\},\\
&\mathbf{H}_{c,0}\coloneqq\{\mathbf{w}\in\mathbf{H}^1(\Omega_c)\mid \mathbf{w}=\mathbf{0}\ \text{on}\ \Gamma_c\},\\
&\mathbf{H}_{c,\mathrm{div}}\coloneqq\{\mathbf{w}\in\mathbf{H}_{c,0}\,|\nabla\cdot\mathbf{w}=0\},\\
&\mathbf{H}_{m,0}\coloneqq\{\mathbf{w}\in\mathbf{H}(\mathrm{div};\Omega_m)\mid \mathbf{w}\cdot\mathbf{n}_m=0\ \text{ on }\ \Gamma_m\},\\
&\mathbf{H}_{m,\mathrm{div}}\coloneqq\{\mathbf{w}\in\mathbf{H}_{m,0}\,|\nabla\cdot\mathbf{w}=0\},\\
&X_m\coloneqq H^1(\Omega_m)\cap L^2_0(\Omega_m).
\end{aligned}
$$

Here $L^2_0(\Omega_m)$ is a subspace of $L^2$ whose elements are of mean zero. We denote $(\cdot,\cdot)_c$, $(\cdot,\cdot)_m$ the inner products on the spaces $L^2(\Omega_c)$, $L^2(\Omega_m)$, respectively (also for the corresponding vector spaces). The inner product on $L^2(\Omega)$ is simply denoted by $(\cdot,\cdot)$. Then it is clear that

$$
(u,v)=(u_m,v_m)_m+(u_c,v_c)_c,\quad \|u\|^2_{L^2(\Omega)}=\|u_m\|^2_{L^2(\Omega_m)}+\|u_c\|^2_{L^2(\Omega_c)},
$$

where $u_m\coloneqq u|_{\Omega_m}$ and $u_c\coloneqq u|_{\Omega_c}$. We will suppress the dependence on the domain in the $L^2$ norm if there is no ambiguity.

For convenience of presentation we introduce the following linear forms:

$$
\mathrm{B}(\mathbf{u},v,w)=\frac{1}{2}\int_\Omega(\mathbf{u}\cdot(w\nabla v)-\mathbf{u}\cdot(v\nabla w))dx. \tag{19}
$$

$$
\mathrm{B}_c(\mathbf{u},\mathbf{v},\mathbf{w})=\frac{1}{2}\int_{\Omega_c}((\mathbf{u}\cdot\nabla\mathbf{v})\mathbf{w}-(\mathbf{u}\cdot\nabla\mathbf{w})\mathbf{v})dx+\frac{1}{2}\int_{\Gamma_{cm}}((\mathbf{u}\cdot\mathbf{w})(\mathbf{v}\cdot\mathbf{n}_{cm})-(\mathbf{u}\cdot\mathbf{v})(\mathbf{w}\cdot\mathbf{n}_{cm}))dS. \tag{20}
$$

$$a_c(\mathbf{u}_c,\mathbf{v}_c)=2(\nu(\varphi_c,\mathrm{T}_c)\mathbb{D}(\mathbf{u}_c),\mathbb{D}(\mathbf{v}_c))_c+\sum_{i=1}^{d-1}\alpha_{BJSJ}\int_{\Gamma_{cm}}\frac{\nu(\varphi_c)}{\sqrt{\mathrm{trace}(\Pi)}}(\mathbf{u}_c\cdot\boldsymbol{\tau}_i)(\mathbf{v}_c\cdot\boldsymbol{\tau}_i)dS. \tag{21}$$

The trilinear terms $\mathrm{B}_c(\mathbf{u},\mathbf{v},\mathbf{w})$ and $\mathrm{B}(\mathbf{u},v,w)$ are antisymmetric formulation (in the weak form) of the advection term in the Navier–Stokes equations and the convection term in the heat equation, respectively, that is,

$$\mathrm{B}_c(\mathbf{u},\mathbf{v},\mathbf{v})=0,\quad \mathrm{B}(\mathbf{u},w,w)=0. \tag{22}$$

These two trilinear terms are defined differently in the integral domains, the presence of integrals along domain interface, as well as the variables (vector vs. scalar).

The following weak form of the CHNSDB system (1)–(14) with temperature of zero mean is introduced in Chen et al. [1], see also Chen et al. [46].

**Definition 1** Suppose that $d=3$ and $\mathcal{T}>0$ is arbitrary (distinguish time $\mathcal{T}$ from temperature $T$ carefully). We consider the initial data $\varphi_0\in H^1(\Omega),\mathbf{u}_c(0)\in\mathbf{H}_{c,\mathrm{div}},\mathbf{u}_m(0)\in\mathbf{H}_{m,\mathrm{div}},T_0\in H^1(\Omega)$. The functions $(\mathbf{u}_c,P_c,\mathbf{u}_m,P_m,T,\varphi,\mu)$ with the following properties

$$\mathbf{u}_c\in L^\infty(0,\mathcal{T};\mathbf{L}^2(\Omega_c))\cap L^2(0,\mathcal{T};\mathbf{H}_{c,0}),\ \frac{\partial\mathbf{u}_c}{\partial t}\in L^{\frac{4}{3}}(0,\mathcal{T};(\mathbf{H}_{c,0})'), \tag{23}$$

$$\mathbf{u}_m\in L^\infty(0,\mathcal{T};\mathbf{L}^2(\Omega_m))\cap L^2(0,\mathcal{T};\mathbf{H}_{m,0}),\ \frac{\partial\mathbf{u}_m}{\partial t}\in L^{\frac{4}{3}}(0,\mathcal{T};(\mathbf{H}_{m,0})'), \tag{24}$$

$$P_c\in L^{\frac{4}{3}}(0,\mathcal{T};L^2(\Omega_c)),\quad P_m\in L^{\frac{4}{3}}(0,\mathcal{T};X_m), \tag{25}$$

$$T\in L^\infty(0,\mathcal{T};L^2(\Omega))\cap L^2(0,\mathcal{T};H^1(\Omega)),T_t\in L^2(0,\mathcal{T};(H^1(\Omega))'), \tag{26}$$

$$\varphi\in L^\infty(0,\mathcal{T};H^1(\Omega))\cap L^2(0,\mathcal{T};H^3(\Omega)),\varphi_t\in L^2(0,\mathcal{T};(H^1(\Omega))'), \tag{27}$$

$$\mu\in L^2(0,\mathcal{T};H^1(\Omega)), \tag{28}$$

is called a finite energy weak solution of the CHNSDB system (1)–(14), if the following conditions are satisfied:

**(1)** For any $\mathbf{v}_c\in\mathbf{H}_{c,0}$ and $q_c\in L^2(\Omega_c)$,

$$\begin{aligned}&\rho_0\langle\partial_t\mathbf{u}_c,\mathbf{v}_c\rangle_c+\rho_0\mathrm{B}_c(\mathbf{u}_c,\mathbf{u}_c,\mathbf{v}_c)+a_c(\mathbf{u}_c,\mathbf{v}_c)-(P_c,\nabla\cdot\mathbf{v}_c)_c\\&+\int_{\Gamma_{cm}}P_m(\mathbf{v}_c\cdot\mathbf{n}_{cm})dS+(\nabla\cdot\mathbf{u}_c,q_c)_c+(\varphi_c\nabla\mu(\varphi_c),\mathbf{v}_c)_c=(\alpha\rho_0gT_c\vec{z},\mathbf{v}_c)_c,\end{aligned} \tag{29}$$

**(2)** For any $\mathbf{v}_m\in\mathbf{H}_{m,0}$ and $q_m\in H^1(\Omega_m)$,

$$\begin{aligned}&\frac{\rho_0}{\chi}\langle\partial_t\mathbf{u}_m,\mathbf{v}_m\rangle_m+(\nu(\varphi_m,T_m)\Pi^{-1}\mathbf{u}_m,\mathbf{v}_m)_m+(\nabla P_m,\mathbf{v}_m)_m-(\mathbf{u}_m,\nabla q_m)_m\\&+(\varphi_m\nabla\mu(\varphi_m),\mathbf{v}_m)_m-\int_{\Gamma_{cm}}\mathbf{u}_c\cdot\mathbf{n}_{cm}q_m\,ds=(\alpha\rho_0gT_m\vec{z},\mathbf{v}_m)_m.\end{aligned} \tag{30}$$

**(3)** For any $W\in H^1(\Omega)$,

$$\langle\partial_tT,W\rangle+B(\mathbf{u},T,W)+(\kappa(T)\nabla T,\nabla W)=0. \tag{31}$$

**(4)** For any $v, \phi \in H^1(\Omega)$,

$$\langle \partial_t \varphi, v\rangle + (\mathrm{M}(\varphi)\nabla\mu(\varphi), \nabla v) - (\mathbf{u}\varphi, \nabla v) = 0, \tag{32}$$

$$\gamma\left[\frac{1}{\varepsilon}(f(\varphi), \phi) + \varepsilon(\nabla\varphi, \nabla\phi)\right] - (\mu(\varphi), \phi) = 0. \tag{33}$$

**(5)** $\varphi|_{t=0} = \varphi_0(x),\ T|_{t=0} = T_0(x),\ \mathbf{u}_c|_{t=0} = \mathbf{u}_c(0),\ \mathbf{u}_m|_{t=0} = \mathbf{u}_m(0).$

Let $\tau > 0$ be the time step and $K = [\mathcal{T}/\tau]$. Set $t^k = k\tau$ for $0 \le k \le K$. We introduce the difference quotient operator $\delta_\tau$ such that $\delta_\tau \varphi_h^{k+1} = \frac{\varphi_h^{k+1} - \varphi_h^k}{\tau}$. Let $\Omega_c^h$ and $\Omega_m^h$ be the quasi-uniform triangulation of the domain $\Omega_c$ and $\Omega_m$ with mesh size $h$ respectively. We assume that $\Omega_c^h$ and $\Omega_m^h$ coincide on the interface $\Gamma_{cm}$. Then $\Omega^h := \Omega_c^h \cup \Omega_m^h$ forms a triangulation of the whole domain $\Omega$. Let $P_r(\mathcal{K})$ be the space of polynomials of degree equal to or less than $r$ on triangle $\mathcal{K} \in \Omega^h$. Then $Y_h$ refers to the finite element approximation of $H^1(\Omega)$ based on the triangulation $\Omega^h$, such as

$$Y_h = \{v_h \in C(\overline{\Omega}) | v_h|_K \in P_r(\mathcal{K}), \forall \mathcal{K} \in \Omega_h\}.$$

Denote by $\mathbf{X}_c^h$ and $M_c^h$ the finite element approximation of $\mathbf{H}_{c,0}$ and $L^2(\Omega_c)$ for the Navier–Stokes velocity and pressure respectively. We assume that $\mathbf{X}_c^h$ and $M_c^h$ satisfy the inf-sup condition, or so-called LBB condition, that

$$\sup_{\mathbf{v}_h \in \mathbf{X}_c^h} \frac{(\nabla \cdot \mathbf{v}_h, q_h)_c}{\|\mathbf{v}_h\|_{H^1}} \ge c\|q_h\|_{L^2}, \qquad \forall q_h \in M_c^h. \tag{34}$$

The classical Taylor–Hood finite element spaces and the Mini finite element spaces are often used for $\mathbf{X}_c^h$ and $M_c^h$ [58]. Similarly, we define $\mathbf{X}_m^h, M_m^h$ to be the finite element spaces of $\mathbf{H}_{m,0}, X_m$ for Darcy velocity and pressure respectively. In addition, we assume $\mathbf{X}_m^h$ and $M_m^h$ satisfy a non-standard inf-sup condition such that

$$\sup_{\mathbf{v}_h \in \mathbf{X}_m^h} \frac{(\mathbf{v}_h, \nabla q_h)_m}{\|\mathbf{v}_h\|_{L^2}} \ge c\|q_h\|_{L^2}, \qquad \forall q_h \in M_m^h. \tag{35}$$

This condition is also supported by the Taylor–Hood finite element spaces.

It is important to note that the element in $M_m^h$—conforming finite element space of $M_m$ for Darcy pressure–is of zero mean, while the element in $M_c^h$ for the approximation of the pressure of the free flow is not subject to this constraint. Well-posedness of a related model (CHSD) with similar conditions imposed on the pressure is discussed in Han et al. [25].

## 2.2 | The scheme based on a modified velocity (Scheme MV)

The schemes designed in Chen et al. [1] are not heat-energy conservative because of the loss of (weak) incompressibility in the numerical solution of the Darcy velocity, compare Equation (42), and the implicit–explicit discretization of the domain interface terms. To compensate the loss of incompressibility, we add back the stabilization terms used in the divergence-free condition, compare Equation (44) below. This leads to the following scheme based on a modified velocity (Scheme MV):

**Step 1** Find $\varphi_h^{k+1} \in Y_h$ and $\mu_h^{k+1} \in Y_h$ such that for any $v_h, \phi_h \in Y_h$,

$$(\delta_\tau \varphi_h^{k+1}, v_h) + (M(\varphi_h^k)\nabla\mu_h^{k+1}, \nabla v_h) - (\overline{\mathbf{u}}_h^{k+1}\varphi_h^k, \nabla v_h) = 0, \tag{36}$$

$$\gamma\left[\frac{1}{\varepsilon}(f(\varphi_h^{k+1}, \varphi_h^k), \phi_h) + \varepsilon(\nabla\varphi_h^{k+1}, \nabla\phi_h)\right] - (\mu_h^{k+1}, \phi_h) = 0, \tag{37}$$

where $f(\varphi_h^{k+1}, \varphi_h^k) = (\varphi_h^{k+1})^3 - \varphi_h^k$, and the intermediate velocity $\overline{\mathbf{u}}_h^{k+1}$ is defined as

$$\overline{\mathbf{u}}^{k+1} = \begin{cases} \overline{\mathbf{u}}_{m,h}^{k+1}, & x \in \Omega_m, \\ \overline{\mathbf{u}}_{c,h}^{k+1}, & x \in \Omega_c, \end{cases} \tag{38}$$

with $\overline{\mathbf{u}}_{m,h}^{k+1}$ and $\overline{\mathbf{u}}_{c,h}^{k+1}$ defined via operator-splitting:

$$\frac{\rho_0}{\chi} \frac{\overline{\mathbf{u}}_{m,h}^{k+1} - \mathbf{u}_{m,h}^k}{\tau} + \varphi_{m,h}^k \nabla \mu_{m,h}^{k+1} = 0, \tag{39}$$

$$\rho_0 \frac{\overline{\mathbf{u}}_{c,h}^{k+1} - \mathbf{u}_{c,h}^k}{\tau} + \varphi_{c,h}^k \nabla \mu_{c,h}^{k+1} = 0. \tag{40}$$

**Step 2** Find $\mathbf{u}_{m,h}^{k+1} \in \mathbf{X}_m^h$ and $P_{m,h}^{k+1} \in M_m^h$ such that for any $\mathbf{v}_{m,h} \in \mathbf{X}_m^h$ and $q_{m,h} \in M_m^h$,

$$\left( \frac{\rho_0}{\chi} \delta_\tau \mathbf{u}_{m,h}^{k+1} + \frac{\nu(\varphi_{m,h}^k, T_{m,h}^k)}{\Pi} \mathbf{u}_{m,h}^{k+1} + \nabla P_{m,h}^{k+1} + \varphi_{m,h}^k \nabla \mu_{m,h}^{k+1}, \mathbf{v}_{m,h} \right)_m = (\alpha \rho_0 g T_h^{k\vec{z}}, \mathbf{v}_{m,h})_m, \tag{41}$$

$$\beta \tau (\nabla P_{m,h}^{k+1}, \nabla q_{m,h})_m - (\mathbf{u}_{m,h}^{k+1}, \nabla q_{m,h})_m - \int_{\Gamma_{cm}} \mathbf{u}_{c,h}^k \cdot \mathbf{n}_{cm} q_{m,h} dS = 0, \tag{42}$$

where $\beta$ is a stabilization parameter to be specified later on.

**Step 3** Find $T_h^{k+1} \in Y_h$ such that for any $W_h \in Y_h$,

$$(\delta_\tau T_h^{k+1}, W_h) + \mathrm{B}(\widetilde{\mathbf{u}}_h^k, T_h^{k+1}, W_h) + (\kappa(T_h^k) \nabla T_h^{k+1}, \nabla W_h) = 0, \tag{43}$$

where

$$\widetilde{\mathbf{u}}_h^k = \begin{cases} \mathbf{u}_{m,h}^{k+1} - \tau \beta \nabla P_{m,h}^{k+1}, & x \in \Omega_m, \\ \mathbf{u}_{c,h}^k, & x \in \Omega_c. \end{cases} \tag{44}$$

**Step 4** Find $\mathbf{u}_{c,h}^{k+1} \in \mathbf{X}_c^h$ and $P_{c,h}^{k+1} \in M_c^h$ such that for any $\mathbf{v}_{c,h} \in \mathbf{X}_c^h$ and $q_{c,h} \in M_c^h$,

$$\begin{aligned} &\rho_0 (\delta_\tau \mathbf{u}_{c,h}^{k+1}, \mathbf{v}_{c,h})_c + \rho_0 \mathrm{B}_c(\mathbf{u}_{c,h}^k, \mathbf{u}_{c,h}^{k+1}, \mathbf{v}_{c,h}) + a_c^k(\mathbf{u}_{c,h}^{k+1}, \mathbf{v}_{c,h}) - (P_{c,h}^{k+1}, \nabla \cdot \mathbf{v}_{c,h})_c \\ &+ (\nabla \cdot \mathbf{u}_{c,h}^{k+1}, q_{c,h})_c + (\varphi_{c,h}^k \nabla \mu_{c,h}^{k+1}, \mathbf{v}_{c,h})_c + \int_{\Gamma_{cm}} P_{m,h}^{k+1} (\mathbf{v}_{c,h} \cdot \mathbf{n}_{cm}) dS \\ &= (\alpha \rho_0 g T_h^{k\vec{z}}, \mathbf{v}_{c,h})_c. \end{aligned} \tag{45}$$

We first establish that the scheme (36)–(45) is conservative.

**Theorem 1** *We have the following theorem. The numerical scheme* (36)–(45) *is conservative in the sense that for* $k = 1, \ldots, (K-1)$ *there holds*

$$\int_\Omega \varphi_h^{k+1} dx = \int_\Omega \varphi_h^k dx = \cdots = \int_\Omega \varphi_h^0 dx, \tag{46}$$

$$\int_\Omega T_h^{k+1} dx = \int_\Omega T_h^k dx = \cdots = \int_\Omega T_h^0 dx = 0, \tag{47}$$

where $\varphi_h^0$ and $T_h^0$ are the finite element approximation of the initial phase field function and the initial temperature, respectively.

*Proof.* The mass conservation (46) follows immediately by taking $v_h = 1$ in Equation (36).

Introduce the average temperature over $\Omega_m$: $\overline{T}_{m,h}^{k+1} = \frac{1}{|\Omega_m|}\int_{\Omega_m} T_h^{k+1} dx$. Taking $q_{m,h} = (T_h^{k+1} - \overline{T}_{m,h}^{k+1})|_{\Omega_m}$ in Equation (42), one obtains

$$(\mathbf{u}_{m,h}^{k+1} - \beta\tau\nabla P_{m,h}^{k+1}, \nabla(T_h^{k+1} - \overline{T}_{m,h}^{k+1}))_m = -\int_{\Gamma_{cm}} \mathbf{u}_{c,h}^k \cdot \mathbf{n}_{cm}(T_h^{k+1} - \overline{T}_{m,h}^{k+1})dS, \tag{48}$$

Evaluating Equation (45) at time level $t_k$, taking $\mathbf{v}_{c,h} = 0$ and $q_{c,h} = T_h^{k+1} - \overline{T}_{m,h}^{k+1}$, and performing integration by parts, one derives

$$(\mathbf{u}_{c,h}^k, \nabla(T_h^{k+1} - \overline{T}_{m,h}^{k+1}))_c = \int_{\Gamma_{cm}} \mathbf{u}_{c,h}^k \cdot \mathbf{n}_{cm}(T_h^{k+1} - \overline{T}_{m,h}^{k+1})dS. \tag{49}$$

Summation of (48) and (49) gives

$$(\mathbf{u}_{m,h}^{k+1} - \beta\tau\nabla P_{m,h}^{k+1}, \nabla(T_h^{k+1} - \overline{T}_{m,h}^{k+1}))_m + (\mathbf{u}_{c,h}^k, \nabla(T_h^{k+1} - \overline{T}_{m,h}^{k+1}))_c = 0.$$

Hence it follows from the definitions (19) and (44) that

$$\begin{aligned} B(\widetilde{\mathbf{u}}_h^k, T_h^{k+1}, 1) &= \frac{1}{2}\int_\Omega \widetilde{\mathbf{u}}_h^k \cdot \nabla T_h^{k+1} dx \\ &= \frac{1}{2}\int_\Omega \widetilde{\mathbf{u}}_h^k \cdot \nabla(T_h^{k+1} - \overline{T}_{m,h}^{k+1}) dx \\ &= 0. \end{aligned}$$

Conservation of the total heat energy (47) then follows from taking $W_h = 1$ in Equation (43). This completes the proof. ∎

Recalling the definition of $A$ from Equation (16), we introduce a modified energy as follows

$$\widetilde{\mathcal{E}}_{mv}^k = \int_{\Omega_c} \frac{\rho_0}{2}|\mathbf{u}_{c,h}^k|^2 dx + \int_{\Omega_m} \frac{\rho_0}{2\chi}|\mathbf{u}_{m,h}^k|^2 dx + \int_\Omega \frac{A}{2}(\mathrm{T}_h^k)^2 dx + E(\varphi_h^k) + A\bar{c}\tau\int_\Omega |\nabla \mathrm{T}_h^k|^2 dx. \tag{50}$$

with $E(\varphi_h^k) := \gamma\int_\Omega \left[\frac{\varepsilon}{2}|\nabla\varphi_h^k|^2 + \frac{1}{\varepsilon}F(\varphi_h^k)\right] dx$. Following the same line of proof as in Chen et al. [1] one can establish the unique solvability and the energy stability of the scheme as follows.

**Proposition 1** *The numerical scheme* (36)–(45) *with sufficiently large* $\beta$ (*depending on the domain and* $\rho_0$, compare *Lemma 1 and Theorem 2 in Chen et al.* [46]) *is unconditionally uniquely solvable at each time step, and it satisfies the following modified energy law*,

$$\begin{aligned} &\widetilde{\mathcal{E}}_{mv}^{k+1} - \widetilde{\mathcal{E}}_{mv}^k + \tau\|\sqrt{\mathrm{M}}\nabla\mu_h^{k+1}\|_{L^2}^2 + \frac{\tau^2}{4\rho_0}(\chi\|\varphi_{m,h}^k\nabla\mu_{m,h}^{k+1}\|^2 + \|\varphi_{c,h}^k\nabla\mu_{c,h}^{k+1}\|^2) \\ &\le -\frac{\gamma\varepsilon}{2}\|\nabla(\varphi_h^{k+1}1 - \varphi_h^k 0)\|_{L^2}^2 - \frac{\rho_0}{12}\|\mathbf{u}_{c,h}^{k+1} - \mathbf{u}_{c,h}^k\|_{L^2}^2 - \frac{\rho_0}{6\chi}\|\mathbf{u}_{m,h}^{k+1} - \mathbf{u}_{m,h}^k\|_{L^2}^2 - \frac{A}{2}\|T_h^{k+1} - T_h^k\|_{L^2}^2, \end{aligned} \tag{51}$$

where $M = M(\varphi_h^k)$, and $A$ is a constant satisfying (16).

### 2.3 | The scheme based on a modified temperature (Scheme MT)

We note that the algorithm (36)–(45) is sequentially decoupled, allowing the Cahn–Hiliard equation, the Darcy equations, the Navier–Stokes equations, and the heat equation to be solved separately but

in an orderly fashion at each time step. Nonetheless the velocity and pressure of the Navier–Stokes solver are still coupled together. The decoupling of the viscous step and pressure gradient is particularly important for solving the Navier–Stokes equations in 3D. On the other hand, due to the domain interface boundary condition (13), the classical pressure projection/correction methods as reviewed in Guermond et al. [59] are not directly applicable. Here in Scheme MT below we adopt a special form of the artificial compressibility method [48, 60] that avoids boundary conditions in the update of pressure, see also DeCaria et al. [61]. Due to the usage of artificial compressibility the temperature field is no longer conservative even with a modified velocity. To maintain the conservation of heat energy, we modify the temperature via a step of post-processing. Specifically the numerical scheme based on a modified temperature (Scheme MT) for solving the CHNSDB model (1)–(14) reads as follows.

**Step 1** find $\varphi_h^{k+1} \in Y_h$ and $\mu_h^{k+1} \in Y_h$ such that for any $v_h, \phi_h \in Y_h$,

$$(\delta_\tau \varphi_h^{k+1}, v_h) + (\mathrm{M}(\varphi_h^k)\nabla \mu_h^{k+1}, \nabla v_h) - (\overline{\mathbf{u}}_h^{k+1}\varphi_h^k, \nabla v_h) = 0, \tag{52}$$

$$\gamma\left[\frac{1}{\varepsilon}(f(\varphi_h^{k+1}, \varphi_h^k), \phi_h) + \varepsilon(\nabla\varphi_h^{k+1}, \nabla\phi_h)\right] - (\mu_h^{k+1}, \phi_h) = 0, \tag{53}$$

where $f(\varphi_h^{k+1}, \varphi_h^k) = (\varphi_h^{k+1})^3 - \varphi_h^k$, and the intermediate velocity $\overline{\mathbf{u}}_h^{k+1}$ is defined as

$$\overline{\mathbf{u}}^{k+1} = \begin{cases} \overline{\mathbf{u}}_{m,h}^{k+1}, & x \in \Omega_m, \\ \overline{\mathbf{u}}_{c,h}^{k+1}, & x \in \Omega_c, \end{cases} \tag{54}$$

with $\overline{\mathbf{u}}_{m,h}^{k+1}$ and $\overline{\mathbf{u}}_{c,h}^{k+1}$ defined via operator-splitting:

$$\frac{\rho_0}{\chi}\frac{\overline{\mathbf{u}}_{m,h}^{k+1} - \mathbf{u}_{m,h}^k}{\tau} + \varphi_{m,h}^k \nabla \mu_{m,h}^{k+1} = 0, \tag{55}$$

$$\rho_0 \frac{\overline{\mathbf{u}}_{c,h}^{k+1} - \mathbf{u}_{c,h}^k}{\tau} + \varphi_{c,h}^k \nabla \mu_{c,h}^{k+1} = 0. \tag{56}$$

**Step 2** Find $\mathbf{u}_{m,h}^{k+1} \in \mathbf{X}_m^h$ and $P_{m,h}^{k+1} \in M_m^h$ such that for any $\mathbf{v}_{m,h} \in \mathbf{X}_m^h$ and $q_{m,h} \in M_m^h$,

$$\left(\frac{\rho_0}{\chi}\delta_\tau \mathbf{u}_{m,h}^{k+1} + \frac{\nu(\varphi_{m,h}^k, T_{m,h}^k)}{\Pi}\mathbf{u}_{m,h}^{k+1} + \nabla P_{m,h}^{k+1} + \varphi_{m,h}^k \nabla \mu_{m,h}^{k+1}, \mathbf{v}_{m,h}\right)_m = (\alpha\rho_0 g T_h^k \vec{z}, \mathbf{v}_{m,h})_m, \tag{57}$$

$$\beta\tau(\nabla P_{m,h}^{k+1}, \nabla q_{m,h})_m - (\mathbf{u}_{m,h}^{k+1}, \nabla q_{m,h})_m - \int_{\Gamma_{cm}} \mathbf{u}_{c,h}^k \cdot \mathbf{n}_{cm} q_{m,h} dS = 0, \tag{58}$$

where $\beta$ is a stabilization parameter to be specified later on.

**Step 3** Find $\widetilde{T}_h^{k+1} \in Y_h$ such that for any $W_h \in Y_h$,

$$\left(\frac{\widetilde{T}_h^{k+1} - T_h^k}{\tau}, W_h\right) + B(\mathbf{u}_h^k, \widetilde{T}_h^{k+1}, W_h) + (\kappa(T_h^k)\nabla\widetilde{T}_h^{k+1}, \nabla W_h) = 0, \tag{59}$$

and obtain the temperature update via post-processing

$$T_h^{k+1} = \widetilde{T}_h^{k+1} - d^{k+1}, \tag{60}$$

with $d^{k+1} = \frac{1}{|\Omega|}\int_\Omega \widetilde{T}_h^{k+1} dx$. This ensures that $T_h^{k+1}$ has zero mean.

**Step 4** Find $\mathbf{u}_{c,h}^{k+1} \in \mathbf{X}_c^h$ and $P_{c,h}^{k+1} \in M_c^h$ such that for any $\mathbf{v}_{c,h} \in \mathbf{X}_c^h$ and $q_{c,h} \in M_c^h$,

$$\begin{aligned}&\rho_0(\delta_\tau \mathbf{u}_{c,h}^{k+1}, \mathbf{v}_{c,h})_c + \rho_0 \mathrm{B}_c(\mathbf{u}_{c,h}^k, \mathbf{u}_{c,h}^{k+1}, \mathbf{v}_{c,h}) + a_c^k(\mathbf{u}_{c,h}^{k+1}, \mathbf{v}_{c,h}) - (2P_{c,h}^k - P_{c,h}^{k-1}, \nabla \cdot \mathbf{v}_{c,h})_c \\ &\quad + \frac{s}{\tau}(\nabla \cdot (\mathbf{u}_{c,h}^{k+1} - \mathbf{u}_{c,h}^k), \nabla \cdot \mathbf{v}_{c,h})_c + (\varphi_{c,h}^k \nabla \mu_{c,h}^{k+1}, \mathbf{v}_{c,h})_c + \int_{\Gamma_{cm}} P_{m,h}^{k+1}(\mathbf{v}_{c,h} \cdot \mathbf{n}_{cm}) dS \\ &\quad = (\alpha \rho_0 g T_h^k \vec{z}, \mathbf{v}_{c,h})_c, \end{aligned} \tag{61}$$

where $s$ is an arbitrary positive stabilizing parameter.

**Step 5** Find $P_{c,h}^{k+1} \in M_c^h$ such that

$$(P_{c,h}^{k+1} - P_{c,h}^k, q_{c,h})_c = -\frac{s}{\tau}(\nabla \cdot \mathbf{u}_{c,h}^{k+1}, q_{c,h})_c, \quad \forall q_h \in M_c^h. \tag{62}$$

Given that $T_h^k \in L_0^2(\Omega)$, it follows from Equation (59) that the constant $d^{k+1}$ is of order $\tau$. Hence $T_h^{k+1}$ is an order $\tau$ correction of $\widetilde{T}_h^{k+1}$, which justifies the consistency of the post-processing step (60). It is clear that the scheme (52)–(62) is conservative.

**Proposition 2** *The numerical scheme (52)–(62) is conservative in the sense that for $k = 1, \dots, (K-1)$ there holds*

$$\int_\Omega \varphi_h^{k+1} dx = \int_\Omega \varphi_h^k dx = \cdots = \int_\Omega \varphi_h^0 dx, \tag{63}$$

$$\int_\Omega T_h^{k+1} dx = \int_\Omega T_h^k dx = \cdots = \int_\Omega T_h^0 dx = 0, \tag{64}$$

*where $\varphi_h^0$ and $T_h^0$ are the finite element approximation of the initial phase field function and the initial temperature, respectively.*

To establish the energy stability, we recall two lemmas.

**Lemma 1** (*Chen et al.* [46]). *Suppose $w \in X_m$, and $\mathbf{v}_{c,h} \in \mathbf{X}_c^h$ satisfy*

$$(\nabla \cdot \mathbf{v}_{c,h}, q_{c,h})_c = 0, \quad \forall q_{c,h} \in M_c^h, \tag{65}$$

*then*

$$\left| \int_{\Gamma_{cm}} \mathbf{v}_{c,h} \cdot \mathbf{n}_{cm} w \, dS \right| \le C \|\nabla w\|_{L^2(\Omega_m)} \|\mathbf{v}_{c,h}\|_{L^2(\Omega_c)}. \tag{66}$$

**Lemma 2** (*Chen et al.* [1]). *Suppose $(\varphi_h^{k+1}, \mu_h^{k+1}, T_h^{k+1}, \mathbf{u}_{c,h}^{k+1}, P_{c,h}^{k+1}, \mathbf{u}_{m,h}^{k+1}, P_{m,h}^{k+1})$, $0 \le k \le K-1$, is a solution to the numerical scheme (52)–(62), and that $A$ satisfies (16). Then for every $0 \le k \le K-1$ there holds*

$$\begin{aligned}&\tau(\alpha \rho_0 g T_{c,h}^k \vec{z}, \mathbf{u}_{c,h}^{k+1})_c + \tau(\alpha \rho_0 g T_{m,h}^k \vec{z}, \mathbf{u}_{m,h}^{k+1})_m \\ &\quad \le A\bar{c}\tau \|\nabla T_h^k\|_{L^2}^2 + \tau a_c^k(\mathbf{u}_{c,h}^{k+1}, \mathbf{u}_{c,h}^{k+1}) + \tau \|\sqrt{\nu_m/\Pi}\mathbf{u}_m^{k+1}\|_{L^2}^2. \end{aligned} \tag{67}$$

Recalling the definition of $A$ from (16), we introduce a modified energy as follows

$$\begin{aligned}\widetilde{\mathcal{E}}_A^k = &\int_{\Omega_c} \frac{\rho_0}{2}|\mathbf{u}_{c,h}^k|^2 dx + \int_{\Omega_m} \frac{\rho_0}{2\chi}|\mathbf{u}_{m,h}^k|^2 dx + \int_\Omega \frac{A}{2}(T_h^k)^2 dx + E(\varphi_h^k) \\ &+ \frac{s}{2}\int_{\Omega_c} |\nabla \cdot \mathbf{u}_{c,h}^k|^2 dx + \frac{\tau^2}{2s}\int_{\Omega_c} |P_{c,h}^k|^2 dx + A\bar{c}\tau \int_\Omega |\nabla T_h^k|^2 dx. \end{aligned} \tag{68}$$

with $E(\varphi_h^k) := \gamma \int_\Omega \left[\frac{\varepsilon}{2}|\nabla \varphi_h^k|^2 + \frac{1}{\varepsilon}F(\varphi_h^k)\right] dx$.

The following theorem establishes the unique solvability and the energy stability of the scheme.

**Theorem 2** *The numerical scheme (52)–(62) with sufficiently large $\beta$ (depending on the domain and $\rho_0$) and arbitrary $s > 0$ is unconditionally uniquely solvable at each time step, and it satisfies the following modified energy law,*

$$\begin{aligned}
&\widetilde{\mathcal{E}}_A^{k+1} - \widetilde{\mathcal{E}}_A^{k} + \tau\|\sqrt{M}\nabla\mu_h^{k+1}\|_{L^2}^2 + \frac{\beta\tau^2}{2}\|\nabla P_{m,h}^{k+1}\|_{L^2}^2 + \frac{\tau^2}{4\rho_0}(\chi\|\varphi_{m,h}^k\nabla\mu_{m,h}^{k+1}\|^2 + \|\varphi_{c,h}^k\nabla\mu_{c,h}^{k+1}\|^2)\\
&\le -\frac{\gamma\varepsilon}{2}\|\nabla(\varphi_h^{k+1}1 - \varphi_h^k 0)\|_{L^2}^2 - \frac{\rho_0}{12}\|\mathbf{u}_{c,h}^{k+1} - \mathbf{u}_{c,h}^k\|_{L^2}^2 - \frac{\rho_0}{6\chi}\|\mathbf{u}_{m,h}^{k+1} - \mathbf{u}_{m,h}^k\|_{L^2}^2 - \frac{A}{4}\|T_h^{k+1} - T_h^k\|_{L^2}^2\\
&\quad - \frac{\tau^2}{2s}\|P_{c,h}^k - P_{c,h}^{k-1}\|_{L^2}^2. \qquad (69)
\end{aligned}$$

where $M = M(\varphi_h^k)$, and $A$ is a constant satisfying (16).

*Proof.* The unique solvability of the scheme follows the same arguments as in References [1, 46]. We omit the details here for conciseness.

We proceed to prove the discrete energy law (69). It follows from convexity that

$$F(\varphi_h^{k+1}) - F(\varphi_h^k) \le f(\varphi_h^{k+1}, \varphi_h^k)(\varphi_h^{k+1} - \varphi_h^k).$$

Taking $v_h = \tau\mu_h^{k+1}$ in Equation (52) and $\phi_h = \varphi_h^{k+1} - \varphi_h^k$ in (53), summing the resultant gives

$$E(\varphi_h^{k+1}) - E(\varphi_h^k) + \tau\|\sqrt{M}\nabla\mu_h^{k+1}\|_{L^2}^2 + \frac{\gamma\varepsilon}{2}\|\nabla(\varphi_h^{k+1} - \varphi_h^k)\|_{L^2}^2 \le \tau(\overline{\mathbf{u}}_h^{k+1}\varphi_h^k, \nabla\mu_h^{k+1}). \qquad (70)$$

In view of the definitions (55) and (56), Equation (70) can be written as

$$\begin{aligned}
&E(\varphi_h^{k+1}) - E(\varphi_h^k) + \tau\|\sqrt{M}\nabla\mu_h^{k+1}\|_{L^2}^2 + \frac{\gamma\varepsilon}{2}\|\nabla(\varphi_h^{k+1} - \varphi_h^k)\|_{L^2}^2\\
&\quad + \frac{\tau^2}{\rho_0}(\chi\|\varphi_{m,h}^k\nabla\mu_{m,h}^{k+1}\|^2 + \|\varphi_{c,h}^k\nabla\mu_{c,h}^{k+1}\|^2) \le \tau(\mathbf{u}_h^k\varphi_h^k, \nabla\mu_h^{k+1}). \qquad (71)
\end{aligned}$$

Next, setting $\mathbf{v}_{m,h} = \tau\mathbf{u}_{m,h}^{k+1}$ in Equation (57) and $q_{m,h} = \tau P_{m,h}^{k+1}$ in (58), summing up the results, one obtains

$$\begin{aligned}
&\frac{\rho_0}{2\chi}\{\|\mathbf{u}_{m,h}^{k+1}\|_{L^2}^2 - \|\mathbf{u}_{m,h}^k\|_{L^2}^2 + \|\mathbf{u}_{m,h}^{k+1} - \mathbf{u}_{m,h}^k\|_{L^2}^2\} + \tau\|\sqrt{\nu_m/\Pi}\mathbf{u}_{m,h}^{k+1}\|_{L^2}^2 + \beta\tau^2\|\nabla P_{m,h}^{k+1}\|_{L^2}^2\\
&\quad + \tau(\mathbf{u}_{m,h}^{k+1}\varphi_{m,h}^k, \nabla\mu_{m,h}^{k+1})_m - \tau\int_{\Gamma_{cm}}\mathbf{u}_{c,h}^k\cdot\mathbf{n}_{cm}P_{m,h}^{k+1}\,dS = \tau(\alpha\rho_0 g\mathrm{T}_{m,h}^k\vec{z}, \mathbf{u}_{m,h}^{k+1})_m. \qquad (72)
\end{aligned}$$

Taking $W_h = A\tau\widetilde{T}_h^{k+1}$ in (59), by the anti-symmetry (22) one has

$$\frac{A}{2}\{\|\widetilde{T}_h^{k+1}\|_{L^2}^2 - \|T_h^k\|_{L^2}^2 + \|\widetilde{T}_h^{k+1} - T_h^k\|_{L^2}^2\} + A\tau\|\sqrt{\kappa}\nabla\widetilde{T}_h^{k+1}\|_{L^2}^2 = 0.$$

It follows from the post-processing step (60).

$$\frac{A}{2}\{\|T_h^{k+1}\|_{L^2}^2 - \|\widetilde{T}_h^{k+1}\|_{L^2}^2 + \|\widetilde{T}_h^{k+1} - T_h^{k+1}\|_{L^2}^2\} = 0,$$

where one has utilized the fact that $T_h^{k+1}$ is of zero mean. Hence

$$\frac{A}{2}\{\|T_h^{k+1}\|_{L^2}^2 - \|T_h^k\|_{L^2}^2 + \|\widetilde{T}_h^{k+1} - T_h^k\|_{L^2}^2 + \|\widetilde{T}_h^{k+1} - T_h^{k+1}\|_{L^2}^2\} + A\tau\|\sqrt{\kappa}\nabla\widetilde{T}_h^{k+1}\|_{L^2}^2 = 0,$$

which implies that

$$\frac{A}{2}\{\|T_h^{k+1}\|_{L^2}^2-\|T_h^k\|_{L^2}^2+\|\widetilde{T}_h^{k+1}-T_h^k\|_{L^2}^2\}+\frac{A}{4}\|\widetilde{T}_h^{k+1}-T_h^{k+1}\|_{L^2}^2+A\tau\|\sqrt{\kappa}\nabla\widetilde{T}_h^{k+1}\|_{L^2}^2\le 0. \tag{73}$$

Likewise, taking $\mathbf{v}_{c,h}=\tau\mathbf{u}_{c,h}^{k+1}$ in Equation (61) gives

$$\begin{aligned}&\frac{\rho_0}{2}\{\|\mathbf{u}_{c,h}^{k+1}\|_{L^2}^2-\|\mathbf{u}_{c,h}^k\|_{L^2}^2+\|\mathbf{u}_{c,h}^{k+1}-\mathbf{u}_{c,h}^k\|_{L^2}^2\}+\tau a_c^k(\mathbf{u}_{c,h}^{k+1},\mathbf{u}_{c,h}^{k+1})\\&\quad+\frac{s}{2}[\|\nabla\cdot\mathbf{u}_{c,h}^{k+1}\|_{L^2}^2-\|\nabla\cdot\mathbf{u}_{c,h}^k\|_{L^2}^2+\|\nabla\cdot(\mathbf{u}_{c,h}^{k+1}-\mathbf{u}_{c,h}^k)\|_{L^2}^2]\\&\quad+\tau\int_{\Gamma_{cm}}P_{m,h}^{k+1}(\mathbf{u}_{c,h}^{k+1}\cdot\mathbf{n}_{cm})dS+\tau(\mathbf{u}_{c,h}^{k+1}\varphi_{c,h}^k,\nabla\mu_{c,h}^{k+1})_c\\&\qquad=\tau(\alpha\rho_0 gT_{c,h}^k\vec{z},\mathbf{u}_{c,h}^{k+1})_c+\tau(2P_{c,h}^k-P_{c,h}^{k-1},\nabla\cdot\mathbf{u}_{c,h}^{k+1})_c.\end{aligned} \tag{74}$$

Now one takes $q_{c,h}=\frac{\tau^2}{s}P_{c,h}^{k+1}$ in Equation (62) to obtain

$$\frac{\tau^2}{2s}[\|P_{c,h}^{k+1}\|_{L^2}^2-\|P_{c,h}^k\|_{L^2}^2+\|P_{c,h}^{k+1}-P_{c,h}^k\|_{L^2}^2]=-\tau(\nabla\cdot\mathbf{u}_{c,h}^{k+1},P_{c,h}^{k+1})_c. \tag{75}$$

Similarly one takes $q_{c,h}=-\frac{\tau^2}{s}(P_{c,h}^{k+1}-2P_{c,h}^k+P_{c,h}^{k-1})$ in Equation (62) to derive

$$\begin{aligned}&-\frac{\tau^2}{2s}[\|P_{c,h}^{k+1}-P_{c,h}^k\|\|_{L^2}^2-\|P_{c,h}^k-P_{c,h}^{k-1}\|\|_{L^2}^2+\|P_{c,h}^{k+1}-2P_{c,h}^k+P_{c,h}^{k-1}\|_{L^2}^2]\\&\quad=\tau(\nabla\cdot\mathbf{u}_{c,h}^{k+1},P_{c,h}^{k+1}-2P_{c,h}^k+P_{c,h}^{k-1})_c.\end{aligned} \tag{76}$$

On the other hand, Equation (62) implies that

$$(P_{c,h}^{k+1}-2P_{c,h}^k+P_{c,h}^{k-1},q_{c,h})_c=-\frac{s}{\tau}(\nabla\cdot(\mathbf{u}_{c,h}^{k+1}-\mathbf{u}_{c,h}^k),q_{c,h})_c,\quad\forall q_h\in M_c^h. \tag{77}$$

Since $P_{c,h}^{k+1}-2P_{c,h}^k+P_{c,h}^{k-1}\in M_c^h$, it follows that

$$\frac{\tau^2}{2s}\|P_{c,h}^{k+1}-2P_{c,h}^k+P_{c,h}^{k-1}\|_{L^2}^2\le\frac{s}{2}\|\nabla\cdot(\mathbf{u}_{c,h}^{k+1}-\mathbf{u}_{c,h}^k)\|_{L^2}^2. \tag{78}$$

Taking summation of (74), (75), (76), and (78), one obtains that

$$\begin{aligned}&\frac{\rho_0}{2}\{\|\mathbf{u}_{c,h}^{k+1}\|_{L^2}^2-\|\mathbf{u}_{c,h}^k\|_{L^2}^2+\|\mathbf{u}_{c,h}^{k+1}-\mathbf{u}_{c,h}^k\|_{L^2}^2\}+\tau a_c^k(\mathbf{u}_{c,h}^{k+1},\mathbf{u}_{c,h}^{k+1})\\&\quad+\frac{s}{2}[\|\nabla\cdot\mathbf{u}_{c,h}^{k+1}\|_{L^2}^2-\|\nabla\cdot\mathbf{u}_{c,h}^k\|_{L^2}^2]+\frac{\tau^2}{2s}[\|P_{c,h}^{k+1}\|_{L^2}^2-\|P_{c,h}^k\|_{L^2}^2+\|P_{c,h}^k-P_{c,h}^{k-1}\|_{L^2}^2]\\&\quad+\tau\int_{\Gamma_{cm}}P_{m,h}^{k+1}(\mathbf{u}_{c,h}^{k+1}\cdot\mathbf{n}_{cm})dS+\tau(\mathbf{u}_{c,h}^{k+1}\varphi_{c,h}^k,\nabla\mu_{c,h}^{k+1})_c\\&\qquad\le\tau(\alpha\rho_0 gT_{c,h}^k\vec{z},\mathbf{u}_{c,h}^{k+1})_c.\end{aligned} \tag{79}$$

Recall the definition of $\mathcal{E}_A$ from Equation (17). Combining the estimates (71), (73), and (79), we obtain

$$\begin{aligned}&\mathcal{E}_A^{k+1}-\mathcal{E}_A^k+\tau\|\sqrt{\mathrm{M}}\nabla\mu_h^{k+1}\|_{L^2}^2+\tau a_c^k(\mathbf{u}_{c,h}^{k+1},\mathbf{u}_{c,h}^{k+1})+\|\sqrt{\nu_m/\Pi}\mathbf{u}_{m,h}^{k+1}\|_{L^2}^2+A\tau\|\sqrt{\kappa}\nabla\widetilde{\mathrm{T}}_h^{k+1}\|_{L^2}^2\\&\quad+\beta\tau^2\|\nabla P_{m,h}^{k+1}\|_{L^2}^2+\frac{\tau^2}{\rho_0}(\chi\|\varphi_{m,h}^k\nabla\mu_{m,h}^{k+1}\|^2+\|\varphi_{c,h}^k\nabla\mu_{c,h}^{k+1}\|^2)+\frac{A}{4}\|\mathrm{T}_h^{k+1}-\mathrm{T}_h^k\|_{L^2}^2\\&\quad+\frac{s}{2}[\|\nabla\cdot\mathbf{u}_{c,h}^{k+1}\|_{L^2}^2-\|\nabla\cdot\mathbf{u}_{c,h}^k\|_{L^2}^2]+\frac{\tau^2}{2s}[\|P_{c,h}^{k+1}\|_{L^2}^2-\|P_{c,h}^k\|_{L^2}^2+\|P_{c,h}^k-P_{c,h}^{k-1}\|_{L^2}^2]\\&\quad+\frac{\gamma\varepsilon}{2}\|\nabla(\varphi_h^{k+1}1-\varphi_h^k0)\|_{L^2}^2+\frac{\rho_0}{2}\|\mathbf{u}_{c,h}^{k+1}-\mathbf{u}_{c,h}^k\|_{L^2}^2+\frac{\rho_0}{2\chi}\|\mathbf{u}_{m,h}^{k+1}-\mathbf{u}_{m,h}^k\|_{L^2}^2\end{aligned}$$

$$\leq -\tau(\mathbf{u}_h^{k+1}-\mathbf{u}_h^k,\varphi_h^k\nabla\mu_h^{k+1})-\tau\int_{\Gamma_{cm}}(\mathbf{u}_{c,h}^{k+1}-\mathbf{u}_{c,h}^k)\cdot\mathbf{n}_{cm}P_{m,h}^{k+1}dS$$
$$+\ \tau(\alpha\rho_0 g\mathrm{T}_{c,h}^k\vec{z},\mathbf{u}_{c,h}^{k+1})_c+\tau(\alpha\rho_0 g\mathrm{T}_{m,h}^k\vec{z},\mathbf{u}_{m,h}^{k+1})_m. \tag{80}$$

Estimates of the four terms on the right-hand side of the inequality (80) follow the same lines as those in Chen et al. [1]. We reproduce the arguments here for completeness. By the Cauchy–Schwarz inequality there holds

$$-\tau(\mathbf{u}_h^{k+1}-\mathbf{u}_h^k,\varphi_h^k\nabla\mu_h^{k+1})\leq\frac{\rho_0}{3}\|\mathbf{u}_{c,h}^{k+1}-\mathbf{u}_{c,h}^k\|_{L^2}^2+\frac{\rho_0}{3\chi}\|\mathbf{u}_{m,h}^{k+1}-\mathbf{u}_{m,h}^k\|_{L^2}^2$$
$$+\frac{3\tau^2}{4\rho_0}(\chi\|\varphi_{m,h}^k\nabla\mu_{m,h}^{k+1}\|^2+\|\varphi_{c,h}^k\nabla\mu_{c,h}^{k+1}\|^2). \tag{81}$$

Lemma 1 yields that

$$-\tau\int_{\Gamma_{cm}}(\mathbf{u}_{c,h}^{k+1}-\mathbf{u}_{c,h}^k)\cdot\mathbf{n}_{cm}P_{m,h}^{k+1}dS\leq C\tau\|\mathbf{u}_{c,h}^{k+1}-\mathbf{u}_{c,h}^k\|_{L^2}\|\nabla P_{m,h}^{k+1}\|_{L^2}$$
$$\leq\frac{\rho_0}{12}\|\mathbf{u}_{c,h}^{k+1}-\mathbf{u}_{c,h}^k\|_{L^2}^2+C_1\tau^2\|\nabla P_{m,h}^{k+1}\|_{L^2}, \tag{82}$$

where $C_1$ depends only on $\Omega_m$, $\Omega_c$, and $\rho_0$. In light of the estimates (81)–(82), and the estimate (67) in Lemma 2, the inequality (80) then becomes

$$\mathcal{E}_A^{k+1}-\mathcal{E}_A^k+\tau\|\sqrt{M}\nabla\mu_h^{k+1}\|_{L^2}^2+\tau a_c^k(\mathbf{u}_{c,h}^{k+1},\mathbf{u}_{c,h}^{k+1})+\tau\|\sqrt{\nu_m/\Pi}\mathbf{u}_{m,h}^{k+1}\|_{L^2}^2+A\tau\|\sqrt{\kappa}\nabla\widetilde{T}_h^{k+1}\|_{L^2}^2$$
$$+\frac{\beta\tau^2}{2}\|\nabla P_{m,h}^{k+1}\|_{L^2}^2+\frac{\tau^2}{4\rho_0}(\chi\|\varphi_{m,h}^k\nabla\mu_{m,h}^{k+1}\|^2+\|\varphi_{c,h}^k\nabla\mu_{c,h}^{k+1}\|^2)+\frac{A}{4}\|T_h^{k+1}-T_h^k\|_{L^2}^2$$
$$+\frac{s}{2}[\|\nabla\cdot\mathbf{u}_{c,h}^{k+1}\|_{L^2}^2-\|\nabla\cdot\mathbf{u}_{c,h}^k\|_{L^2}^2]+\frac{\tau^2}{2s}[\|P_{c,h}^{k+1}\|_{L^2}^2-\|P_{c,h}^k\|_{L^2}^2+\|P_{c,h}^k-P_{c,h}^{k-1}\|_{L^2}^2]$$
$$+\frac{\gamma\epsilon}{2}\|\nabla(\varphi_h^{k+1}1-\varphi_h^k0)\|_{L^2}^2+\frac{\rho_0}{12}\|\mathbf{u}_{c,h}^{k+1}-\mathbf{u}_{c,h}^k\|_{L^2}^2+\frac{\rho_0}{6\chi}\|\mathbf{u}_{m,h}^{k+1}-\mathbf{u}_{m,h}^k\|_{L^2}^2$$
$$\leq A\bar{c}\tau\|\nabla T_h^k\|_{L^2}^2+\tau a_c^k(\mathbf{u}_{c,h}^{k+1},\mathbf{u}_{c,h}^{k+1})+\tau\|\sqrt{\nu_m/\Pi}\mathbf{u}_m^{k+1}\|_{L^2}^2+C_1\tau^2\|\nabla P_{m,h}^{k+1}\|_{L^2}^2. \tag{83}$$

Since

$$\beta\geq 2C_1,\quad A\bar{c}\tau\|\nabla T_h^k\|_{L^2}^2\leq A\tau\|\sqrt{\kappa}\nabla T_h^k\|_{L^2}^2,\quad \|\sqrt{\kappa}\nabla\widetilde{T}_h^{k+1}\|_{L^2}^2=\|\sqrt{\kappa}\nabla T_h^{k+1}\|_{L^2}^2,$$

we obtain the following modified discrete energy law

$$\widetilde{\mathcal{E}}_A^{k+1}-\widetilde{\mathcal{E}}_A^k+\tau\|\sqrt{M}\nabla\mu_h^{k+1}\|_{L^2}^2+\frac{\beta\tau^2}{2}\|\nabla P_{m,h}^{k+1}\|_{L^2}^2+\frac{\tau^2}{4\rho_0}(\chi\|\varphi_{m,h}^k\nabla\mu_{m,h}^{k+1}\|^2+\|\varphi_{c,h}^k\nabla\mu_{c,h}^{k+1}\|^2)$$
$$\leq-\frac{\gamma\epsilon}{2}\|\nabla(\varphi_h^{k+1}1-\varphi_h^k0)\|_{L^2}^2-\frac{\rho_0}{12}\|\mathbf{u}_{c,h}^{k+1}-\mathbf{u}_{c,h}^k\|_{L^2}^2-\frac{\rho_0}{6\chi}\|\mathbf{u}_{m,h}^{k+1}-\mathbf{u}_{m,h}^k\|_{L^2}^2-\frac{A}{4}\|T_h^{k+1}-T_h^k\|_{L^2}^2$$
$$-\frac{\tau^2}{2s}\|P_{c,h}^k-P_{c,h}^{k-1}\|_{L^2}^2.$$

This completes the proof. ∎

## 3 | NUMERICAL RESULTS

In this section, we present numerical evidence that our schemes are conservative, unconditionally stable, and accurate. All the numerical experiments are performed using the software FreeFem++ [62]. For convenience, we test the algorithm in a two-dimension domain: $\Omega_m=[0,1]\times[0,1]$, $\Omega_c=[0,1]\times[-1,0]$, $\Omega=\Omega_m\cup\Omega_c=[0,1]\times[-1,1]$, and $\Gamma_{cm}=[0,1]\times\{0\}$. Throughout we take $\nu(\varphi,\mathrm{T})$

**TABLE 1** Value of parameters in conservation test

| Parameters | $\kappa$ | $\rho_0$ | $\chi$ | $\nu_c$ | $\nu_m$ | $\Pi$ | $M$ (Mobility) | $\gamma$ | $\varepsilon$ | $\alpha_{BJSJ}$ | $\beta$ | $\alpha$ | $g$ |
|---|---|---|---|---|---|---|---|---|---|---|---|---|---|
| Value | $0.001/(4\pi^2)$ | 1 | 1 | 0.1 | 0.1 | $0.1\,\mathbb{I}_2$ | 0.1 | 0.1 | 0.1 | $\sqrt{0.1}$ | 1 | 0.01 | 10 |

*Note*: $\mathbb{I}_2$ represents the two-dimensional unit matrix.

**TABLE 2** Comparison of the non-conservative scheme from [1] to Scheme MV in terms of the absolute value of the relative error (84)

| $\tau$ | Scheme [1] | Scheme MV |
|---|---|---|
| $\frac{1}{4}$ | $1.03E-01$ | $8.16E-17$ |
| $\frac{1}{8}$ | $2.49E-02$ | $4.20E-16$ |
| $\frac{1}{16}$ | $5.65E-03$ | $3.97E-17$ |
| $\frac{1}{32}$ | $1.36E-03$ | $3.33E-16$ |
| $\frac{1}{64}$ | $3.39E-04$ | $5.62E-16$ |
| $\frac{1}{128}$ | $8.55E-05$ | $1.25E-16$ |
| $\frac{1}{256}$ | $2.15E-05$ | $5.82E-16$ |
| $\frac{1}{512}$ | $5.41E-06$ | $2.94E-16$ |
| $\frac{1}{1024}$ | $1.36E-06$ | $3.82E-16$ |

to be constant, and the stabilization parameter $s = 1$. We have tested both Scheme MV and Scheme MT where Scheme MV is also employed for initialization of Scheme MT. Qualitatively similar results are obtained for both schemes. For conciseness, we only report results generated by Scheme MV. We refer to our earlier work [1] for more extensive results of numerical simulations.

### 3.1 | Conservation of the total heat energy

We numerically verify that Scheme MV (36)–(45) is conserving the total heat energy under the condition of no differential heating at the boundary. The value of parameters in the PDE system are showed in Table 1.

The manufactured solution is constructed as follows.

$$\begin{aligned}&\varphi = 0, \quad T = 2 + \exp(-0.0001t)\cos(2\pi x),\\ &\mathbf{u}_m = \mathbf{u}_c = 0,\\ &P_m = P_c = \exp(-0.0001t)\cos(2\pi x).\end{aligned}$$

In the numerical experiment we set $h = \frac{1}{64}$, vary the time-step $\tau = \frac{1}{4}, \frac{1}{8}, \ldots, \frac{1}{1024}$, and calculate the relative error

$$\left|\frac{\int_\Omega T_h^2 - T_h^0 dx}{\int_\Omega T_h^0}\right|. \tag{84}$$

The results computed using $T_h^j, j \geq 2$ are similar. In Table 2, we compare the results generated by the scheme in Chen et al. [1] to those by the conservative scheme (36)–(45). It shows that the relative error of the total heat energy by the current conservative scheme remains within machine accuracy, while the scheme in Chen et al. [1] is not conservative though the relative error is decreasing as the time-step size refines.

TABLE 3 Convergence test $\tau = h$, final time $T = 1$

| $h$ | | 1/8 | 1/16 | 1/32 | 1/64 | 1/128 |
|---|---|---|---|---|---|---|
| $P_m$ | $L^2$ error | 0.516059 | 0.347221 | 0.196211 | 0.104213 | 0.0538113 |
| | Order | | 0.571682 | 0.823448 | 0.912871 | 0.953554 |
| $P_c$ | $L^2$ error | 0.630284 | 0.409013 | 0.224568 | 0.116382 | 0.0591389 |
| | Order | | 0.623855 | 0.864994 | 0.948284 | 0.976689 |
| $\varphi$ | $L^2$ error | 1.06778 | 0.619019 | 0.341222 | 0.180327 | 0.0928443 |
| | Order | | 0.786559 | 0.859273 | 0.920095 | 0.957730 |
| $T$ | $L^2$ error | 0.0107169 | 0.00651675 | 0.00366849 | 0.00195186 | 0.0010073 |
| | Order | | 0.717663 | 0.828966 | 0.910337 | 0.954356 |
| $\mathbf{u}_c$ | $L^2$ error | 0.0198353 | 0.00918967 | 0.00496118 | 2.81E-03 | 1.52E-03 |
| | Order | | 1.10999 | 0.889330 | 0.819672 | 0.883234 |
| $\mathbf{u}_m$ | $L^2$ error | 0.28469 | 0.119129 | 0.0534077 | 0.0255947 | 0.0126277 |
| | Order | | 1.25687 | 1.15740 | 1.06120 | 1.01925 |

### 3.2 | Convergence test

Now we demonstrates the accuracy of Scheme MV by methods of manufactured solution. The parameters in the PDE system mostly take identical values as in Table 1, except $\kappa = 0.001$.

The manufactured solutions are the same as in Chen et al. [1]: for $t \in [0, \mathcal{T}]$,

$$\varphi = e^{-t}\cos(\pi x)\cos(\pi y), \quad (x, y) \in \Omega, \tag{85}$$

$$T = 2 + e^{-t}\cos(\pi x)\cos(\pi y), \quad (x, y) \in \Omega, \tag{86}$$

$$\begin{cases} \mathbf{u}_j = e^{-t}\begin{pmatrix} -\frac{1}{2}\sin^2(\pi x)\sin(\pi(y+1)) \\ \sin(2\pi x)\sin^2\left(\frac{\pi(y+1)}{2}\right) \end{pmatrix}, & (x, y) \in \Omega_j, \\ P_j = \frac{1}{\pi}e^{-t}\sin^2(\pi x)\sin^2(\pi y), & (x, y) \in \Omega_j, \end{cases} \quad j \in \{c, m\}. \tag{87}$$

We test the temporal convergence setting $\tau = h$. The $P2 - P1$ finite element pair is used for velocity and pressure, and $P1$ finite element is employed for the approximation of order parameter and temperature. We calculate the relative error of the numerical solution at $t = \mathcal{T} = 1$. The $L^2$ error and the convergence order is reported in Table 3. First order convergence rate is observed for all variables which is further illustrated in Figure 2.

### 3.3 | Stability

In this section we numerically validate that Scheme MV satisfies a discrete energy law. The parameters in the PDE system are set as in Table 4. The initial conditions are $\varphi_0 = 0.2 + 0.4y$, $T_0 = -xy$, and.

$$\mathbf{u}_j(0) = \begin{pmatrix} -\frac{1}{2}\sin^2(\pi x)\sin(\pi(y+1)) \\ \sin(2\pi x)\sin^2\left(\frac{\pi(y+1)}{2}\right) \end{pmatrix}, \quad (x, y) \in \Omega_j, \ \ j \in \{c, m\}, \tag{88}$$

which satisfies $\nabla \cdot \mathbf{u}_0 = 0$. We take the mesh size $h = \frac{1}{64}$ and the time step $\tau = \frac{1}{64}$. We let the constant $A$ to be 100 so that it satisfies the condition (16). In Figure 3, we compare evolution of the discrete

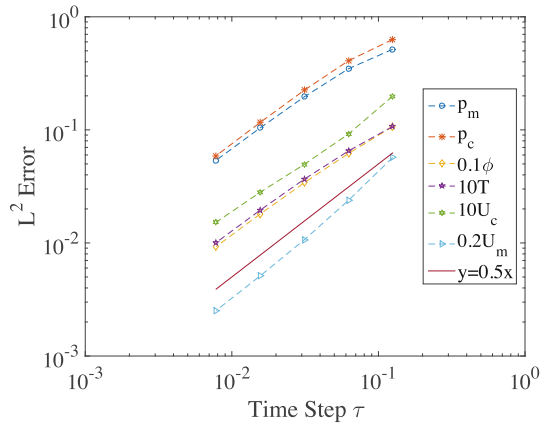


**FIGURE 2** Plot of the $L^2$ error as a function of time-step size: $\tau = h$, final time $T = 1$

**TABLE 4** Parameters in the discrete energy experiments

| PDE parameters | $\alpha$ | $\kappa$ | $\rho_0$ | $\chi$ | $\nu_c$ | $\nu_m$ | $\Pi$ | $M$ (Mobility) | $\gamma$ | $\varepsilon$ | $\alpha_{BJSJ}$ | $\beta$ | $g$ |
|---|---|---|---|---|---|---|---|---|---|---|---|---|---|
| Value in test | 0.5 | $1e^{-3}$ | 1 | 1 | 0.1 | 0.1 | $0.1\mathbb{I}_2$ | 0.1 | 0.1 | 0.1 | $\sqrt{0.1}$ | 1 | 10 |

*Note*: $\mathbb{I}_2$ represents the two-dimensional unit matrix.

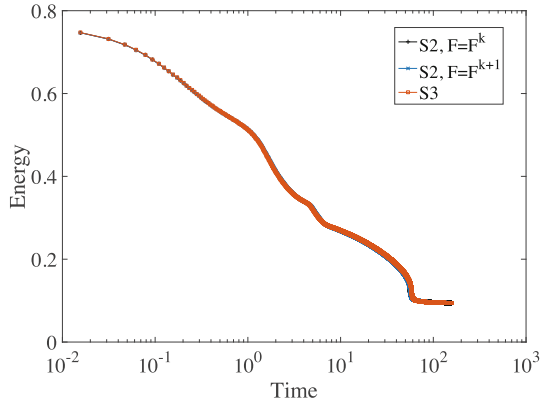


**FIGURE 3** Evolution of discrete energy with the constant $A = 100$. The three energy curves are visibly identical and monotonically deceasing

energy computed by the scheme (36)–(45) (referred to as S3) to those by the two schemes proposed in our earlier work [1] (referred to as S2) where the buoyancy term is discretized explicitly ($F = F^k$) and implicitly ($F = F^{k+1}$), respectively. We observe that the discrete energy curves are virtually identical and monotonically decreasing.

## 4 | CONCLUSIONS

We proposed two mass and heat energy conservative, unconditionally stable, decoupled numerical algorithms for solving the CHNSDB system that models thermal convection of two-phase flows

in superposed free flow and porous media. The schemes totally decouples the computation of the Cahn–Hilliard equation, the Darcy equations, the heat equation, and the Navier–Stokes equations at each time step, thus significantly reducing the computational cost. The second scheme also decouples the computation of the velocity and the pressure of the Navier–Stokes equations. The key ideas in the design include operator splitting, pressure stabilization and artificial compression, and div-grad stabilization. We rigorously show that the schemes are conservative and energy-law preserving. Numerical results confirm the properties of conservation, accuracy and stability of the algorithms. The development of a second-order, unconditionally stable, decoupled scheme will be dealt with in a future work.

## DATA AVAILABILITY STATEMENT

The data that support the findings of this study are available from the corresponding author upon reasonable request.

## ORCID

*Wenbin Chen* https://orcid.org/0000-0001-8305-0764
*Xiaoming Wang* https://orcid.org/0000-0002-2399-6336

## REFERENCES

[1] C. Wenbin, H. Daozhi, X. Wang, and Z. Yichao, *Uniquely solvable and energy stable decoupled numerical schemes for the Cahn-Hilliard-Navier-stokes-Darcy-Boussinesq system*, J. Sci. Comput. 85(2) (2020), 45.
[2] M. Bayani Cardenas, *Hyporheic zone hydrologic science: A historical account of its emergence and a prospectus*, Water Resour. Res. 51(5) (2015), 3601–3616.
[3] D. Marco and Q. Alfio, *Navier-Stokes/Darcy coupling: Modeling, analysis, and numerical approximation*, Rev. Mat. Complut. 22(2) (2009), 315–426.
[4] W. J. Layton, S. Friedhelm, and Y. Ivan, *Coupling fluid flow with porous media flow*, SIAM J. Numer. Anal. 40(6) (2002), 2195–2218.
[5] C. Yanzhao, G. Max, H. Fei, and X. Wang, *Coupled Stokes-Darcy model with Beavers-Joseph interface boundary condition*, Commun. Math. Sci. 8(1) (2010), 1–25.
[6] C. Nan, G. Max, and X. Wang, *Asymptotic analysis of the differences between the Stokes-Darcy system with different interface conditions and the Stokes-Brinkman system*, J. Math. Anal. Appl. 368(2) (2010), 658–676.
[7] C. Wenbin, G. Max, H. Fei, and X. Wang, *A parallel Robin-Robin domain decomposition method for the Stokes-Darcy system*, SIAM J. Numer. Anal. 49(3) (2011), 1064–1084.
[8] C. Wenbin, G. Max, S. Dong, and X. Wang, *Efficient and long-time accurate second-order methods for the Stokes-Darcy system*, SIAM J. Numer. Anal. 51(5) (2013), 2563–2584.
[9] G. Vivette and R. Béatrice, *DG approximation of coupled Navier-Stokes and Darcy equations by Beaver-Joseph-Saffman interface condition*, SIAM J. Numer. Anal. 47(3) (2009), 2052–2089.
[10] F. Chen and C. F. Chen, *Convection in superposed fluid and porous layers*, J. Fluid Mech. 234 (1992), 97–119.
[11] B. Straughan, *Effect of property variation and modelling on convection in a fluid overlying a porous layer*, Int. J. Numer. Anal. Methods Geomech. 26(1) (2001), 75–97.
[12] M. Carr, *Penetrative convection in a superposed porous-medium-fluid layer via internal heating*, J. Fluid Mech. 509 (2004), 305–329.
[13] M. H. Chang, *Thermal convection in superposed fluid and porous layers subjected to a horizontal plane Couette flow*, Phys. Fluids 17(6) (2005), 064106.
[14] M. H. Chang, *Thermal convection in superposed fluid and porous layers subjected to a plane Poiseuille flow*, Phys. Fluids 18(3) (2006), 035104 10.
[15] A. A. Hill and B. Straughan, *Poiseuille flow in a fluid overlying a porous medium*, J. Fluid Mech. 603 (2008), 137–149.
[16] S. C. Hirata, B. Goyeau, D. Gobin, M. Chandesris, and D. Jamet, *Stability of natural convection in superposed fluid and porous layers: Equivalence of the one- and two-domain approaches*, Int. J. Heat Mass Transf. 52(1) (2009), 533–536.
[17] A. A. Hill and B. Straughan, *Global stability for thermal convection in a fluid overlying a highly porous material*, Proc. R. Soc. Lond. Ser. A Math. Phys. Eng. Sci 465(2101) (2009), 207–217.

[18] A. A. Hill and M. Carr, *Nonlinear stability of the one-domain approach to modelling convection in superposed fluid and porous layers*, Proc. R. Soc. Lond. Ser. A Math. Phys. Eng. Sci. 466(2121) (2010), 2695–2705.
[19] S. P. Suma, Y. H. Gangadharaiah, R. Indira, and I. S. Shivakumara, *Throughflow effects on penetrative convection in superposed fluid and porous layers*, Transp. Porous Media 95(1) (2012), 91–110.
[20] T. P. Lyubimova and E. A. Kolchanova, *The onset of double-diffusive convection in a superposed fluid and porous layer under high-frequency and small-amplitude vibrations*, Transp. Porous Media 122(1) (2018), 97–124.
[21] M. McCurdy, N. Moore, and X. Wang, *Convection in a coupled free flow-porous media system*, SIAM J. Appl. Math. 79(6) (2019), 2313–2339.
[22] H. Daozhi, Q. Wang, and X. Wang, *Dynamic transitions and bifurcations for thermal convection in the superposed free flow and porous media*, Phys. D 414 (2020), 132687.
[23] C. Jie, S. Shuyu, and X.-P. Wang, *A numerical method for a model of two-phase flow in a coupled free flow and porous media system*, J. Comput. Phys. 268 (2014), 1–16.
[24] H. Daozhi, S. Dong, and X. Wang, *Two-phase flows in karstic geometry*, Math. Methods Appl. Sci. 37(18) (2014), 3048–3063.
[25] H. Daozhi, X. Wang, and H. Wu, *Existence and uniqueness of global weak solutions to a Cahn-Hilliard-Stokes-Darcy system for two phase incompressible flows in karstic geometry*, J. Differ. Equ. 257(10) (2014), 3887–3933.
[26] C. M. Elliott and A. M. Stuart, *The global dynamics of discrete semilinear parabolic equations*, SIAM J. Numer. Anal. 30(6) (1993), 1622–1663.
[27] D. J. Eyre, *Unconditionally gradient stable time marching the Cahn-Hilliard equation*, Mater. Res. Soc. Sympos. Proc., vol. 529, MRS, Warrendale, PA, 1998, pp. 39–46.
[28] J. Shen, C. Wang, X. Wang, and M. Wise Steven, *Second-order convex splitting schemes for gradient flows with Ehrlich-Schwoebel type energy: Application to thin film epitaxy*, SIAM J. Numer. Anal. 50(1) (2012), 105–125.
[29] G. Karl and O. Saulo, *Improving the accuracy of convexity splitting methods for gradient flow equations*, J. Comput. Phys. 315 (2016), 52–64.
[30] F. Guillén-González and G. Tierra, *On linear schemes for a Cahn-Hilliard diffuse interface model*, J. Comput. Phys. 234 (2013), 140–171.
[31] X. Yang, Z. Jia, and Q. Wang, *Numerical approximations for the molecular beam epitaxial growth model based on the invariant energy quadratization method*, J. Comput. Phys. 333 (2017), 104–127.
[32] X. Yang and J. Lili, *Linear and unconditionally energy stable schemes for the binary fluid-surfactant phase field model*, Comput. Methods Appl. Mech. Eng. 318 (2017), 1005–1029.
[33] G. Yuezheng, Z. Jia, and Q. Wang, *Arbitrarily high-order linear energy stable schemes for gradient flow models*, J. Comput. Phys. 419 (2020), 109610.
[34] J. Shen, J. Xu, and J. Yang, *The scalar auxiliary variable (SAV) approach for gradient flows*, J. Comput. Phys. 353 (2018), 407–416.
[35] J. Shen, J. Xu, and J. Yang, *A new class of efficient and robust energy stable schemes for gradient flows*, SIAM Rev. 61(3) (2019), 474–506.
[36] K. Junseok, K. Kyungkeun, and L. John, *Conservative multigrid methods for Cahn-Hilliard fluids*, J. Comput. Phys. 193(2) (2004), 511–543.
[37] Q. He, G. Roland, and X.-P. Wang, *A least-squares/finite element method for the numerical solution of the Navier-Stokes-Cahn-Hilliard system modeling the motion of the contact line*, J. Comput. Phys. 230(12) (2011), 4991–5009.
[38] F. Xiaobing and W. Steven, *Analysis of a Darcy-Cahn-Hilliard diffuse interface model for the Hele-Shaw flow and its fully discrete finite element approximation*, SIAM J. Numer. Anal. 50(3) (2012), 1320–1343.
[39] H. Daozhi and X. Wang, *A second order in time, uniquely solvable, unconditionally stable numerical scheme for Cahn–Hilliard–Navier–Stokes equation*, J. Comput. Phys. 290 (2015), 139–156.
[40] J. Shen and X. Yang, *Decoupled, energy stable schemes for phase-field models of two-phase incompressible flows*, SIAM J. Numer. Anal. 53(1) (2015), 279–296.
[41] H. Daozhi, *A decoupled unconditionally stable numerical scheme for the Cahn-Hilliard-Hele-Shaw system*, J. Sci. Comput. 66(3) (2016), 1102–1121.
[42] E. Diegel Amanda, W. Cheng, W. Xiaoming, and M. Wise Steven, *Convergence analysis and error estimates for a second order accurate finite element method for the Cahn–Hilliard–Navier–Stokes system*, Numer. Math. 137(3) (2017), 1–40.
[43] Z. Jia, X. Yang, G. Yuezheng, and Q. Wang, *A novel linear second order unconditionally energy stable scheme for a hydrodynamic* Q*-tensor model of liquid crystals*, Comput. Methods Appl. Mech. Eng. 318 (2017), 803–825.
[44] Z. Guo, P. Lin, J. Lowengrub, and S. M. Wise, *Mass conservative and energy stable finite difference methods for the quasi-incompressible Navier-Stokes-Cahn-Hilliard system: Primitive variable and projection-type schemes*, Comput. Methods Appl. Mech. Eng. 326 (2017), 144–174.
[45] G. Yuezheng, Z. Jia, X. Yang, and Q. Wang, *Fully discrete second-order linear schemes for hydrodynamic phase field models of binary viscous fluid flows with variable densities*, SIAM J. Sci. Comput. 40(1) (2018), B138–B167.

[46] C. Wenbin, H. Daozhi, and X. Wang, *Uniquely solvable and energy stable decoupled numerical schemes for the Cahn-Hilliard-Stokes-Darcy system for two-phase flows in karstic geometry*, Numer. Math. 137(1) (2017), 229–255.
[47] C. A. Joel, *Numerical solution of the Navier-Stokes equations*, Math. Comput. 22 (1968), 745–762.
[48] T. Roger, *Une méthode d'approximation de la solution des équations de Navier-Stokes*, Bull. Soc. Math. France. 96 (1968), 115–152.
[49] M. Sebastian, *An unconditionally stable uncoupled scheme for a triphasic Cahn-Hilliard/Navier-Stokes model*, Numer. Methods Partial Differ. Equ. 29(2) (2013), 584–618.
[50] J. Zhao, Second-order decoupled energy-stable schemes for Cahn-Hilliard-Navier-Stokes equations. *arXiv:2103.02210*. 2021;.
[51] Z. Yang and S. Dong, *A roadmap for discretely energy-stable schemes for dissipative systems based on a generalized auxiliary variable with guaranteed positivity*, J. Comput. Phys. 404 (2020), 109121.
[52] X. Yang, *A novel fully-decoupled, second-order and energy stable numerical scheme of the conserved Allen-Cahn type flow-coupled binary surfactant model*, Comput. Methods Appl. Mech. Eng. 373 (2021), 113502.
[53] X. Li, J. Shen and Z. Liu, *New SAV-pressure correction methods for the Navier-Stokes equations: Stability and error analysis*, Math. Comput. (2021), 1. http://dx.doi.org/10.1090/mcom/3651.
[54] J. Zhao, A general framework to derive linear, decoupled and energy-stable schemes for reversible-irreversible thermodynamically consistent models: Part I incompressible hydrodynamic models. *arXiv:2103.02203*. 2021.
[55] C. Wenbin, L. Yuan, C. Wang, and M. Wise Steven, *Convergence analysis of a fully discrete finite difference scheme for the Cahn-Hilliard-Hele-Shaw equation*, Math. Comput. 85(301) (2016), 2231–2257.
[56] L. Yuan, C. Wenbin, C. Wang, and M. Wise Steven, *Error analysis of a mixed finite element method for a Cahn-Hilliard-Hele-Shaw system*, Numer. Math. 135(3) (2017), 679–709.
[57] W. Chen, D. Han, C. Wang, S. Wang, X. Wang, Y. Zhang, Error estimate of a decoupled numerical scheme for the Cahn-Hilliard-Stokes-Darcy system. *arXiv:2106.03260*. 2021; to appear in *IMA Journal of Numerical Analysis*.
[58] G. Vivette and R. Pierre-Arnaud, Theory and algorithms, in *Finite element methods for Navier-Stokes equations*, Springer Series in Computational Mathematics, Vol 5, Springer-Verlag, Berlin, 1986.
[59] J. L. Guermond, P. Minev, and S. Jie, *An overview of projection methods for incompressible flows*, Comput. Methods Appl. Mech. Eng 195(44–47) (2006), 6011–6045.
[60] J. Shen, *On a new pseudocompressibility method for the incompressible Navier-Stokes equations*, Appl. Numer. Math. 21(1) (1996), 71–90.
[61] D. C. Victor, L. William, and M. L. Michael, *A conservative, second order, unconditionally stable artificial compression method*, Comput. Methods Appl. Mech. Eng. 325 (2017), 733–747.
[62] F. Hecht, *New development in freefem++*, J. Numer. Math. 20(3–4) (2012), 251–265.

**How to cite this article:** W. Chen, D. Han, X. Wang, and Y. Zhang, *Conservative unconditionally stable decoupled numerical schemes for the Cahn–Hilliard–Navier–Stokes–Darcy–Boussinesq system*, Numer. Methods Partial Differ. Eq. **38** (2022), 1823–1842. https://doi.org/10.1002/num.22841